



Control of cardiac alternans in a mapping model with memory

Elena G. Tolkacheva^{a,*}, Mónica M. Romeo^b, Daniel J. Gauthier^{a,c}

^a Department of Physics and Center for Nonlinear and Complex Systems, Duke University, Durham, NC 27708 USA

^b Department of Mathematics and Center for Nonlinear and Complex Systems, Duke University, Durham, NC 27708 USA

^c Department of Biomedical Engineering and Center for Nonlinear and Complex Systems, Duke University, Durham, NC 27708 USA

Received 16 October 2003; received in revised form 3 March 2004; accepted 16 March 2004

Communicated by J.P. Keener

Abstract

A generic feature of cardiac muscle is that the duration of an action potential depends on the long-term history of previous action potentials, known as cardiac ‘memory’. Even though memory is known to be an important physiological response, there have only been limited studies of its effect on cardiac dynamics. Here, we investigate a map-based model of paced myocardium in the presence of closed-loop feedback control. The model relates the duration of an action potential to the preceding diastolic interval as well as the preceding action potential duration and thus has some degree of memory. We find that the range of parameters over which control is effective can be enlarged or reduced by memory, a prediction that is independent of the specific functional form of the map. Our work suggests that modifying the degree of memory (e.g., pharmacological agents) with some form of feedback control may be an effective strategy for the maintenance of normal cardiac function.

© 2004 Elsevier B.V. All rights reserved.

PACS: 87.19.Hh; 87.10.+e; 05.45.–a

Keywords: Alternans; Control of alternans; Mapping model; Memory

1. Introduction

Sudden cardiac death, primarily caused by ventricular arrhythmias, is a major public health problem: it is one of the leading causes of mortality in the western world. A possible precursor of some arrhythmias is the beat-to-beat variation of the cardiac electrical excitation occurring at fast heart rates [1,2]. This variation appears as a sequence of long-short-long-short cycles (termed alternans) in important physiological characteristics such as action potential duration (APD) and conduction time. A focus of recent theoretical and

experimental studies is to investigate the mechanisms causing alternans and to terminate this response pattern using closed-loop feedback methods developed by the nonlinear dynamics community. Suppressing such alternans may then prevent the onset of fibrillation [3].

Over the last few years, several studies have demonstrated that alternans can be suppressed with dynamic feedback control of the pacing interval [4–8]. Control of alternans in the conduction time across the atrioventricular (AV) node has been demonstrated in both in vitro rabbit hearts [5] and in vivo human hearts [8]. The observed AV-nodal alternans are known to be well described by a one-dimensional map-based mathematical model [8]. The model can be used to predict the

* Corresponding author. Fax: +1-9196602525.

E-mail address: lena@phy.duke.edu (E.G. Tolkacheva).

range of control parameters that stabilize the desired response patterns.

Recently, Hall and Gauthier [4] demonstrated successful control of cardiac muscle alternans in small pieces of in vitro paced bullfrog cardiac muscle. Understanding how to control muscle is important because it is the primary substrate for fibrillation. It was expected to be more difficult to control cardiac muscle alternans because past research suggests that muscle dynamics is more complicated than AV-nodal dynamics. In particular, several experimental and theoretical studies [9–18] indicate that higher-dimensional behavior (so-called cardiac memory effects) is present in all cardiac tissue to some degree and thus has to be taken into account in order to correctly predict the onset and control of alternans. In general, the presence of memory means that the APD depends not only on the preceding diastolic interval (DI) but also on the previous history of the paced cardiac tissue. The effect of memory seems to be a generic feature of cardiac muscle since it has been reported for humans [19] and different types of animals including pigs [12], rabbits [13], dogs [14–17], and frogs [4].

The primary purpose of this paper is to investigate the effect of memory on control of cardiac alternans. Specifically, we analyze a map-based model of paced cardiac muscle that contains some degree of memory in the presence of closed-loop feedback control. We find that the domain of control can encompass large or small feedback gains depending on the amount of memory. Our results demonstrate that memory effects can enhance the effectiveness of control under the appropriate conditions. This may lead eventually to the development of methods for in vivo control of whole-heart functions.

2. Mapping models with and without memory

2.1. Mapping model without memory

To set the stage for understanding the behavior of the higher-dimensional model, we first consider a simpler one-dimensional map that contains no memory. This mapping model is given by [20,21]

$$A_{n+1} = f(D_n), \quad (1)$$

where A_{n+1} is the APD generated by the $(n + 1)$ th stimulus, and D_n is the n th DI. We illustrate a typical bifurcation diagram in Fig. 1a. Note that the tissue has a stable 1:1 response pattern (every stimulus elicits an action potential of equal duration) for long pacing intervals (slow pacing rate). As the pacing interval decreases (faster pacing), the 1:1 response becomes unstable and a transition to alternans (2:2 response) occurs.¹ For the 1:1 and 2:2 responses considered herein, the pacing relation between APD and DI is $D_n = B - A_n$, where B is the basic pacing interval.

For this simple model, the transition from 1:1 to 2:2 behavior shown in the Fig. 1a can be understood by investigating the restitution properties of the cardiac membrane. Specifically, to predict the pacing rates at which the 1:1 response is stable, one constructs the restitution curve (RC) by plotting APD as a function f of the preceding DI, as in Eq. (1). Nolasco and Dahlen [20] proposed that the transition to alternans occurs when the slope of the RC is equal to unity. However, recent studies [4,9,22–24] have shown that the slope of the RC at the onset of alternans can be significantly larger than unity and thus this criterion fails to predict the existence of alternans in some cases. Later in the paper, we analyze the map (1), independently of the specific form of the function f , in the presence of closed-loop feedback control.

2.2. Mapping model with memory

In contrast to the memoryless model (1), a cardiac mapping model of the form

$$A_{n+1} = F(A_n, D_n) \quad (2)$$

has some amount of memory because it relates the duration of the next action potential both to the previous DI and to the previous APD, i.e., the history of the dynamical system. The general form of this model was first introduced by Otani and Gilmour [15] to explain

¹ Note that the magnitude of the alternans presented in Fig. 1a is considerably larger than the magnitude observed in most experiments.

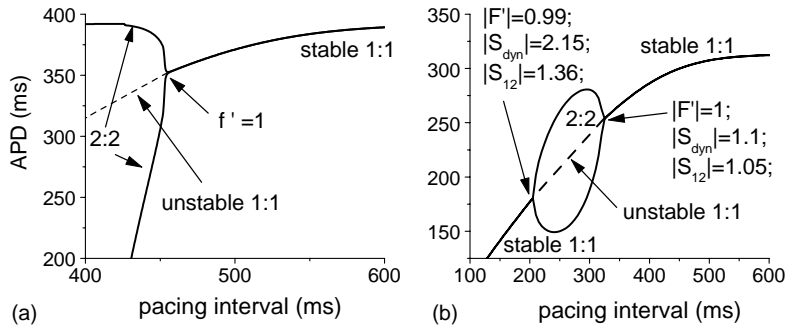


Fig. 1. Bifurcation diagrams showing existence of alternans for (a) the memoryless mapping model (1) and (b) the mapping model (2) with memory. Arrows indicate the points where slopes are determined. Dashed lines show unstable 1:1 response. For (a) $f(D_n) = A_1 - A_2 \exp(-D_n/\tau)$, where $A_1 = 392$ ms, $A_2 = 525.3$ ms, and $\tau = 40$ ms [4]. For the mapping model (2), a specific form of the function F is taken from Refs. [24,25], where all parameters have their typical values except $\tau_{\text{open}} = 50$ ms.

empirical observations from paced dog cardiac Purkinje fibers. More recently, a specific form of F was derived analytically [25] from a three-current ionic model [26].

Our analysis of the model (2) shows that it displays rate-dependent restitution so that there exist two primary types of RCs (the dynamic and S1-S2 RCs), which can be measured independently using different pacing protocols [24]. In the *dynamic pacing protocol*, the pacing interval B_1 is held fixed until the tissue reaches equilibrium, and then progressively shortened. This yields pairs of steady-state values (A^* , D^*) for each B_1 . In the *S1-S2 pacing protocol*, a premature stimulus (“S2”) is delivered at an interval B_2 after pacing the tissue with a sufficiently large number of “S1” stimuli at a pacing interval B_1 so that the tissue reaches equilibrium. The S1-S2 RC is determined by measuring the resulting APD for various coupling intervals B_2 . Experimental studies have shown that the S1-S2 and dynamic RCs differ significantly, and have different slopes (denoted as S_{12} and S_{dyn} , respectively). This is consistent with the predictions of the mapping model (2). The transition to alternans is governed by the combination of the slopes S_{dyn} and S_{12} , so that alternans can exist when

$$|F'| = \left| 1 - S_{12} - \frac{S_{12}}{S_{\text{dyn}}} \right| \geq 1, \quad (3)$$

where F' is the full derivative of F with respect to A_n , evaluated at a fixed point [24]. Note that $S_{12} = S_{\text{dyn}}$ when there is no memory in the model, and that

they differ substantially when there is large memory. A typical bifurcation diagram showing alternans in the mapping model (2) is presented in Fig. 1b, where the slopes of the RCs are different and do not equal unity at the onset of alternans.

3. Control of alternans in the mapping models with and without memory

We now consider the control of alternans in both models (1) and (2). To suppress alternans and stabilize the 1:1 pattern, we adjust the pacing period by an amount given by

$$\varepsilon_n = -\gamma(A_{n-1} - A_{n-2}), \quad (4)$$

where γ is the feedback gain, following the technique² described in Ref. [4]. Control is initiated by adjusting the basic pacing interval B by ε_n .

3.1. Control of alternans in the mapping model without memory

Applying the control technique to the mapping model (1) yields

$$A_{n+1} = f(D_n(A_n, \varepsilon_n)), \quad (5)$$

² Note that the domain of control for the proposed technique is not greatly affected if you can only shorten the inter-beat interval. In fact, the domain of control actually applies to more highly unstable states [27,28].

where $D_n(A_n, \varepsilon_n) = B + \varepsilon_n - A_n$. The linearization of Eq. (5) in a neighborhood of the fixed point (when $A_n = A^*$ and $\varepsilon_n = 0$) is

$$A_{n+1} = A^* + \left. \left(\frac{df}{dD_n} \frac{\partial D_n}{\partial A_n} \right) \right|_{f.p.} (A_n - A^*) + \left. \left(\frac{df}{dD_n} \frac{\partial D_n}{\partial \varepsilon_n} \right) \right|_{f.p.} \varepsilon_n, \tag{6}$$

where f.p. denotes evaluation at the fixed point. We define

$$\mu \equiv \left. \left(\frac{df}{dD_n} \frac{\partial D_n}{\partial A_n} \right) \right|_{f.p.}. \tag{7}$$

Since the controlled pacing relation is $D_n = B + \varepsilon_n - A_n$, then $\partial D_n / \partial A_n = -1$, and thus $df/dD_n = -\mu$. Since $\partial D_n / \partial \varepsilon_n = 1$, then the third term in Eq. (6) is $(df/dD_n)(\partial D_n / \partial \varepsilon_n)|_{f.p.} = -\mu$.

We rewrite Eqs. (4) and (6) in matrix form as

$$\begin{pmatrix} \delta_{n+1} \\ \theta_{n+1} \\ \alpha_{n+1} \end{pmatrix} = \begin{pmatrix} \mu & -\gamma\mu & 0 \\ -1 & 0 & 1 \\ 1 & 0 & 0 \end{pmatrix} \begin{pmatrix} \delta_n \\ \theta_n \\ \alpha_n \end{pmatrix}, \tag{8}$$

where $\delta_n = A_n - A^*$, $\theta_n = \varepsilon_n / \gamma$, and $\alpha_n = \delta_{n-1}$. Control is successful when the eigenvalues of Eq. (8) fall within the unit circle in the complex plane. To find the boundaries of the parameter region where this occurs, we note that the characteristic equation for the eigenvalues λ of Eq. (8) is

$$\lambda^3 - \mu\lambda^2 - \sigma\lambda + \sigma = 0, \tag{9}$$

where $\sigma = \mu\gamma$. Since Eq. (9) has real coefficients, an eigenvalue can exit the unit circle (as μ and σ

vary) in one of three ways: $\lambda = 1$, $\lambda = -1$, or it and its complex conjugate have unit modulus. Substituting $\lambda = \pm 1$ into Eq. (9) yields the first and second boundaries. For the third boundary, we consider the general form of a cubic polynomial with roots $e^{\pm i\varphi}$ for $\varphi \in [0, 2\pi)$ and $\alpha \in \mathbb{R}$:

$$\lambda^3 - (2 \cos \varphi + \alpha)\lambda^2 + (1 + 2\alpha \cos \varphi)\lambda - \alpha = 0. \tag{10}$$

By equating the coefficients of Eqs. (9) and (10) and solving for γ as a function of μ , we obtain the third boundary. The three curves that bound the region where control is successful are

$$\begin{aligned} \mu = 1, \quad \gamma &= \frac{1 + \mu}{2\mu}, \\ \gamma &= \frac{1 - \mu - \sqrt{(1 - \mu)^2 + 4}}{2\mu}, \end{aligned} \tag{11}$$

as shown in Fig. 2a. Condition (11) defines the domain of control for the mapping model (1). Note that the domain does *not* depend on the specific functional form of f , but only on the value of its derivative μ evaluated at the fixed point. Alternans may exist in the uncontrolled mapping model (1) when $\mu \leq -1$. The domain of control indicates the values of the gain γ that should be used to establish control of alternans for different values of the Floquet multiplier μ , which describes the stability of the map in the absence of control. Note that the gain necessary to establish control in the region where alternans exist in the absence of control is small ($0 < \gamma < \sqrt{2} - 1$). This is in contradiction with the experimental observations presented in Ref. [4] where

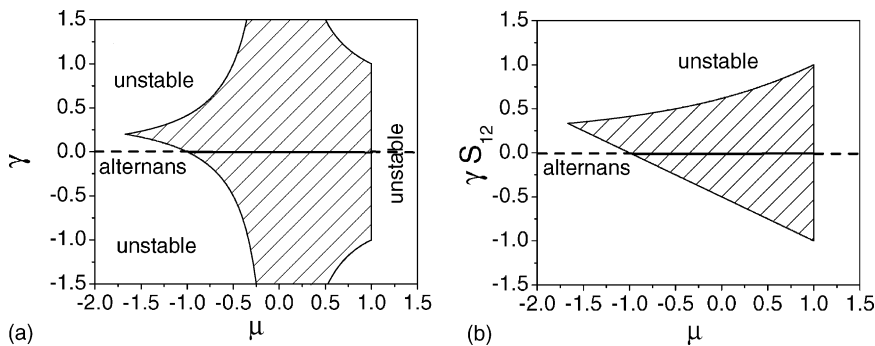


Fig. 2. Domains of control of alternans (shaded region) for (a) the memoryless model (1) and (b) the model with memory (2). Solid (dashed) horizontal lines represent stable (unstable) regions of the uncontrolled systems. Alternans may exist in the absence of control when $\mu \leq -1$.

successful control of alternans in small pieces of paced bullfrog ventricles was demonstrated. It was shown there that the feedback gain γ can be as large as 4.

3.2. Control of alternans in the mapping model with memory

We perform a similar analysis on the mapping model (2) with memory. In the presence of control, Eq. (2) becomes

$$A_{n+1} = F(A_n, D_n(A_n, \varepsilon_n)). \quad (12)$$

Linearizing Eq. (12) in a neighborhood of the fixed point, we find that

$$A_{n+1} = A^* + F'(A_n - A^*) + \left(\frac{\partial F}{\partial D_n} \frac{\partial D_n}{\partial \varepsilon_n} \right) \Big|_{f.p.} \varepsilon_n, \quad (13)$$

where

$$F' = \left(\frac{\partial F}{\partial A_n} + \frac{\partial F}{\partial D_n} \frac{\partial D_n}{\partial A_n} \right) \Big|_{f.p.}.$$

We define

$$\mu = F' \quad \text{and} \quad \frac{\partial F}{\partial D_n} \Big|_{f.p.} = S_{12}. \quad (14)$$

As in Eq. (7), we again define μ as a derivative of F , evaluated at the fixed point. As seen from Eq. (3), the condition for the existence of alternans in the absence of control is given by $\mu \leq -1$. The stability of the 1:1 response pattern under closed-loop feedback control depends on both μ and S_{12} . Each plays a particular role in the stability of the controlled steady state. The value of μ dictates the stability of the uncontrolled steady-state response of the tissue; whereas S_{12} characterizes the immediate response of the tissue to small perturbations, as was shown in Ref. [24]. Note that μ and S_{12} are related through the relationship $\mu = (\partial F/\partial A_n)|_{f.p.} - S_{12}$.

We can rewrite expressions (4) and (13) in matrix form, using the same local variables as in Eq. (8):

$$\begin{pmatrix} \delta_{n+1} \\ \theta_{n+1} \\ \alpha_{n+1} \end{pmatrix} = \begin{pmatrix} \mu & \gamma S_{12} & 0 \\ -1 & 0 & 1 \\ 1 & 0 & 0 \end{pmatrix} \begin{pmatrix} \delta_n \\ \theta_n \\ \alpha_n \end{pmatrix}. \quad (15)$$

The only difference between the matrices describing the controlled dynamics for the maps with and without memory is the term containing the control gain γ . In the memoryless mapping model (1), the magnitude of perturbation sensitivity is proportional to the full derivative μ , whereas it is proportional to the slope S_{12} of the S1-S2 RC in the mapping model with memory (2). When there is no memory, $S_{12} = -\mu$, whereas they can differ substantially when memory is present.

To find the boundaries of the parameter region where control is successful, we again use that the characteristic equation for the eigenvalues λ of Eq. (15) is Eq. (9), but with $\sigma = -\gamma S_{12}$. The three curves that bound the region where control is successful are

$$\begin{aligned} \mu = 1, \quad \gamma S_{12} &= -\frac{1}{2}(\mu + 1), \\ \gamma S_{12} &= -\frac{1}{2}(1 - \mu - \sqrt{(1 - \mu)^2 + 4}). \end{aligned} \quad (16)$$

Similar to the previous model, the domain of control (16) does not depend on the specific form of the function F . We only need to know the values of the full derivative μ and the slope of the S1-S2 RC S_{12} (evaluated at the fixed point) to determine whether it is possible to establish control. Fig. 2b depicts the domain of control for the one-dimensional mapping model with memory (2) according to conditions (16). It can be seen from Fig. 2b that the value of γS_{12} necessary to establish control for this region is relatively small ($0 < \gamma S_{12} < \sqrt{2} - 1$). However, the actual control gain γ can be larger or smaller than this range depending on the value of S_{12} and thus on the amount of memory. Note that Eq. (16) representing the domain of control for the mapping model (2) becomes Eq. (11) if we take $S_{12} = -\mu$. In this case, the domain of control displayed in Fig. 2b can be represented using the same axes as in Fig. 2a, and both domains of control would be equal. Our predictions are consistent with our earlier expectations that S_{12} influences the effects of control since it quantifies the response of the tissue (in equilibrium) to a sudden perturbation, which the controller attempts to cancel.

Stable 1:1 behavior is expected in the region $-1 < \mu < 1$ in the absence of control. The presence of control can, however, destabilize the 1:1 state as can be seen from Fig. 2. The advantage of applying control

when the 1:1 state is stable was discussed in Ref. [4], where successful control of alternans in small pieces of bullfrog muscles was demonstrated.

Comparing our predictions to experiments is not possible at this time because no experiments have measured the slope of the S1-S2 RC *evaluated at the fixed point*.³ Most of the experiments (see, for instance, Refs. [16,17]) used S1-S2 pacing protocol in which the “S1” interval was either fixed or set to only a few different values. Instead, to obtain the domain of control, we need to know the slope of the S1-S2 RC S_{12} at each point on the dynamic RC (i.e., for different S1). The value S_{12} can be greater or less than one, depending on the specific form of F or the specific type of tissue. For example, $S_{12} > 1$ for the function F used to generate the plot shown in Fig. 1b. Hence, the control gain γ must be less than $(\sqrt{2} - 1)$ to be in the region where control is effective. However, preliminary, experiments with bullfrog cardiac muscle indicates that S_{12} can be relatively small (less than 0.4 and as small as 0.05) at the onset of alternans [29] and thus the control gain could be large.

4. Discussion

Thus, the experimentally measured domain of control may be consistent with the predictions of the controlled map with memory (2) if S_{12} is truly less than one in bullfrog. The map without memory (1) does not agree with experiments as demonstrated by Fig. 2a and as noted previously in Ref. [4]. Our analysis is the first to suggest that memory effects may substantially enlarge the domain of control, regulated by S_{12} .

A limitation of our analysis is that we studied the simplest type of cardiac mapping models with memory (so-called “short-term” memory) in which the APD depends on both the previous APD and previous DI. However, some studies indicate that “long-term” memory effects are present in real cardiac tissue [17] that might be described using a “long-term” memory mapping model [9,18]. In this model, the APD

is a function of the two preceding DIs as well as the preceding APD. The dynamic properties of these *two* models can be completely different depending on the parameter values considered. In particular, a “short-term” memory mapping model may exhibit three different RCs, whereas “long-term” memory mapping model may display four RCs. The condition for alternans and its control in a “long-term” mapping model of the form of [9,18] are considered in [30].

Future experiments are needed to determine what specific form of memory the different types of cardiac tissue display and thus what type of mapping models would describe their dynamics. Nevertheless, our results indicate the importance of memory in the control of alternans.

Acknowledgements

We gratefully acknowledge the support of the National Science Foundation under Grants PHY-0243584, DMS-9983320 (M.M.R.), and National Institutes of Health under Grant RO1 HL-72831.

References

- [1] A. Karma, Electrical alternans and spiral wave breakup in cardiac tissue, *Chaos* 4 (1994) 461–472.
- [2] R.F. Gilmour Jr., D.R. Chialvo, Editorial: electrical restitution, critical mass and the riddle of fibrillation, *J. Cardiovasc. Electrophysiol.* 10 (1999) 1087–1089.
- [3] B. Echebarria, A. Karma, Spatiotemporal control of cardiac alternans, *Chaos* 12 (2002) 923.
- [4] G.M. Hall, D.J. Gauthier, Experimental control of cardiac muscle alternans, *Phys. Rev. Lett.* 88 (2002) 198102–198105.
- [5] K. Hall, D.J. Christini, M. Tremblay, J.J. Collins, L. Glass, J. Billette, Dynamic control of cardiac alternans, *Phys. Rev. Lett.* 78 (1997) 4518–4521.
- [6] W.-J. Rappel, F. Fenton, A. Karma, Spatiotemporal control of wave instabilities in cardiac tissue, *Phys. Rev. Lett.* 83 (1999) 456–459.
- [7] D.J. Gauthier, J.E.S. Socolar, Analysis and comparison of multiple-delay schemes for controlling unstable fixed points of discrete maps, *Phys. Rev. E* 57 (1998) 6589–6595.
- [8] D.J. Christini, K.M. Stein, S.M. Markowitz, S. Mittal, D.J. Slotwiner, M.A. Scheiner, S. Iwai, B.B. Lerman, Nonlinear-dynamical arrhythmia control in humans, *Proc. Natl. Acad. Sci.* 98 (2001) 5827.
- [9] J.J. Fox, E. Bodenschatz, R.F. Gilmour, Period-doubling instability and memory in cardiac tissue, *Phys. Rev. Lett.* 89 (2002) 138101.

³ We note that a pacing protocol has been suggested in Ref. [24] for easily determining S_{dyn} , S_{12} , and F' (evaluated at the fixed points) in experiments.

- [10] F.H. Fenton, S.J. Evans, H.M. Hastings, Memory in an excitable medium: a mechanism for spiral wave breakup in the low-excitability limit, *Phys. Rev. Lett.* 83 (1999) 3964–3967.
- [11] E.M. Cherry, F.H. Fenton, Suppression of alternans and conduction blocks despite steep APD restitution: electrotonic, memory and conduction velocity restitution effects, *AJP Heart Circ. Physiol.*, in press.
- [12] L.S. Gettes, G.N. Morehouse, B. Surawicz, Effect of premature depolarization on the duration of action potentials in Purkinje and ventricular fibers of the moderator band of the pig heart. Role of proximity and the duration of the preceding action potential, *Circ. Res.* 30 (1972) 55–66.
- [13] C.L. Gibbs, E.A. Johnson, Effect of changes in frequency of stimulation upon rabbit ventricular action potential, *Circ. Res.* 9 (1961) 165–170.
- [14] V. Elharrar, B. Surawicz, Cycle length effect on restitution of action potential duration in dog cardiac fibers, *Am. J. Physiol.* 244 (1983) H782–H792.
- [15] N.F. Otani, R.F. Gilmour Jr., Memory models for the electrical properties of local cardiac systems, *J. Theor. Biol.* 187 (1997) 409–436.
- [16] R.F. Gilmour Jr., N.F. Otani, M.A. Watanabe, Memory and complex dynamics in cardiac Purkinje fibers, *Am. J. Physiol.* 272 (1997) H1826–H1832.
- [17] M.A. Watanabe, M.L. Koller, Mathematical analysis of dynamics of cardiac memory and accommodation: theory and experiment, *Am. J. Physiol.* 282 (2002) H1534–H1547.
- [18] D.R. Chialvo, D.C. Michaels, J. Jalife, Supernormal excitability as a mechanism of chaotic dynamics of activation in cardiac Purkinje fibers, *Circ. Res.* 66 (1990) 525–545.
- [19] M.R. Franz, C.D. Swerdlow, L.B. Liem, J. Schaefer, Cycle length dependence of human action potential duration in vivo: effects of single extrastimuli, sudden sustained rate acceleration and deceleration, and different steady-state frequencies, *J. Clin. Invest.* 82 (1988) 972–979.
- [20] J.B. Nolasco, R.W. Dahlen, A graphic method for the study of alternation in cardiac action potentials, *J. Appl. Physiol.* 25 (1968) 191–196.
- [21] M. Guevara, G. Ward, A. Shrier, L. Glass, Electrical alternans and period-doubling bifurcations, *IEEE Comp. Cardiol.* 562 (1984) 167–170.
- [22] G.M. Hall, S. Bahar, D.J. Gauthier, Prevalence of rate-dependent behaviors in cardiac muscle, *Phys. Rev. Lett.* 82 (1999) 2995–2998.
- [23] I. Banville, R.A. Gray, Effect of action potential duration and conduction velocity restitution and their spatial dispersion on alternans and the stability of arrhythmias, *J. Cardiovasc. Electrophysiol.* 13 (2002) 1141–1149.
- [24] E.G. Tolkacheva, D.G. Schaeffer, D.J. Gauthier, W. Krassowska, Condition for alternans and stability of the 1:1 response pattern in a “memory” model of paced cardiac dynamics, *Phys. Rev. E* 67 (2003) 031904–031910.
- [25] E.G. Tolkacheva, D.G. Schaeffer, D.J. Gauthier, C.C. Mitchell, Analysis of the Fenton-Karma model through approximation by a one-dimensional map, *Chaos* 12 (2002) 1034–1042.
- [26] F. Fenton, A. Karma, Vortex dynamics in three-dimensional continuous myocardium with fiber rotation: filament instability and fibrillation, *Chaos* 8 (1998) 20–47.
- [27] D.J. Gauthier, J.E.S. Socolar, Comment on “Dynamic control of cardiac alternans”, *Phys. Rev. Lett.* 79 (1997) 4938.
- [28] K. Hall, D.J. Christini, Restricted feedback control of one-dimensional map, *Phys. Rev. E* 63 (2001) 046204.
- [29] S.S. Kalb, H. Dobrovolny, E.G. Tolkacheva, S.F. Idriss, W. Krassowska, D.J. Gauthier, Restitution portrait: a new method for investigating rate-dependence restitution, *JCE*, in press.
- [30] E.G. Tolkacheva, M.M. Romeo, M. Guerraty, D.J. Gauthier, Condition for alternans and its control in a two-dimensional mapping model of paced cardiac dynamics, *PRE.* 69 (2004) 031904.